THE JOURNAL OF BIOLOGICAL CHEMISTRY VOL. 291, NO. 21, pp. 11385–11393, May 20, 2016

Catalytically Active Guanylyl Cyclase B Requires Endoplasmic Reticulum-mediated Glycosylation, and Mutations That Inhibit This Process Cause Dwarfism*

Received for publication, November 12, 2015, and in revised form, March 14, 2016 Published, JBC Papers in Press, March 15, 2016, DOI 10.1074/jbc.M115.704015

Deborah M. Dickey[‡], Aaron B. Edmund[‡], Neil M. Otto[‡], Thomas S. Chaffee[‡], Jerid W. Robinson[‡], and Lincoln R. Potter[‡§1]

From the Departments of [‡]Biochemistry, Molecular Biology, and Biophysics and [§]Pharmacology, University of Minnesota, Minneapolis, Minnesota 55455

C-type natriuretic peptide activation of guanylyl cyclase B (GC-B), also known as natriuretic peptide receptor B or NPR2, stimulates long bone growth, and missense mutations in GC-B cause dwarfism. Four such mutants (L658F, Y708C, R776W, and G959A) bound ^{125}I-C-type natriuretic peptide on the surface of cells but failed to synthesize cGMP in membrane GC assays. Immunofluorescence microscopy also indicated that the mutant receptors were on the cell surface. All mutant proteins were dephosphorylated and incompletely glycosylated, but dephosphorylation did not explain the inactivation because the mutations inactivated a "constitutively phosphorylated" enzyme. Tunicamycin inhibition of glycosylation in the endoplasmic reticulum or mutation of the Asn-24 glycosylation site decreased GC activity, but neither inhibition of glycosylation in the Golgi by *N*-acetylglucosaminyltransferase I gene inactivation nor PNGase F deglycosylation of fully processed GC-B reduced GC activity. We conclude that endoplasmic reticulum-mediated glycosylation is required for the formation of an active catalytic, but not ligand-binding domain, and that mutations that inhibit this process cause dwarfism.

C-type natriuretic peptide (CNP)[2] is a paracrine factor that stimulates long bone growth and axonal path finding and inhibits meiosis in the oocyte (1–3). The biologic signaling receptor for CNP is guanylyl cyclase B (GC-B) (4–6).

GC-B is a homo-oligomer, possibly a dimer, containing a glycosylated extracellular ligand-binding domain, a single membrane-spanning region, and intracellular kinase homology, dimerization, and C-terminal catalytic domains (7). Phosphorylation of the region leading into and at the beginning of the kinase homology domain is required for CNP activation of GC-B, and dephosphorylation inactivates the enzyme (8–14).

Homozygous inactivating mutations in GC-B result in acromesomelic dysplasia, type Maroteaux (AMDM) dwarfism (15–18), and heterozygous inactivating mutations in GC-B cause non-pathological reductions in stature (19). Heterozygous inactivating mutations in GC-B are also associated with short stature observed in Léri-Weill dyschondrosteosis (20). Conversely, genetic mutations that increase GC-B activity result in skeletal overgrowth (21–23).

At least 29 unique inactivating missense mutations in GC-B have been identified in humans (15–19, 24–27). These mutations are randomly distributed from the N terminus (Pro-32) to the C terminus (G959A) of the enzyme, consistent with two potential mechanisms. The first involves multiple processes like disruption of CNP or GTP binding to the enzyme. The second more general mechanism involves conformational changes in the structure of GC-B that preclude catalytic domain formation or activation.

Previous investigators reported that 11 of 12 (25), two of three (26, 27), or one of two (24) missense mutations inhibited the transport of GC-B to the cell surface because of defective cellular trafficking and retention in the ER, as indicated by reduced immunofluorescence imaging of GC-B associated with the plasma membrane. Thus, the current model is that AMDM mutations disrupt intracellular trafficking of GC-B.

Here we characterized four intracellular missense AMDM mutations in GC-B. In contrast to previous reports, we found that all mutants were on the cell surface. However, the GC activity of each mutant was severely reduced or abolished. The mutant receptors migrated as incompletely glycosylated species when fractionated by SDS-PAGE, and inhibition of glycosylation in the ER, but not in the Golgi, produced enzymes with similarly reduced catalytic activity.

Experimental Procedures

Reagents—^{125}I-cGMP radioimmunoassay kits and ^{125}I-CNP-22 were from Perkin Elmer Life Sciences. Non-radioactive natriuretic peptides were from Sigma. ProQ Diamond dye and wheat germ agglutinin were from Life Technologies. Tunicamycin was from Millipore Corp. (Billerica, MA).

Cell Culture, Transfections, and cDNAs—293T-GC-B cells were maintained as described previously (28). GnT1 293 cells lacking the Golgi *N*-acetylglucosaminyltransferase I enzyme (29) were purchased from the ATCC (Manassas, VA). 293T cells were transfected using the calcium/phosphate method as

* This work was supported by National Institutes of Health Grants R01GM098309 (to L. R. P.) and T32AR050938 (to A. B. E.) and the Fund for Science. The authors declare that they have no conflicts of interest with the contents of this article. The content is solely the responsibility of the authors and does not necessarily represent the official views of the National Institutes of Health.

[1] To whom correspondence should be addressed: University of Minnesota, Twin Cities, 6-155 Jackson Hall, 321 Church St. SE, Minneapolis, MN 55455. Tel.: 612-624-7251; E-mail: potter@umn.edu.

[2] The abbreviations used are: CNP, C-type natriuretic peptide; GC, guanylyl cyclase; AMDM, acromesomelic dysplasia, type Maroteaux; ER, endoplasmic reticulum; ANP, atrial natriuretic peptide.

described previously (30). For HeLa cells, a 1:2 mass ratio of plasmid DNA to Lipofectimine2000 was incubated in 0.5 ml of Opti-MEM for 20 min before addition to cells. The mutants used for CNP binding and guanylyl cyclase assays were generated in the rat cDNA backbone. The mutants used for the immunofluorescence studies were generated in the HA-tagged human GC-B cDNA (16).

Immunofluorescence—HeLa cells were fixed with 4% formaldehyde in PBS for 15 min at room temperature and stained for the plasma membrane with wheat germ agglutinin 594 at 5 μg/ml for 10 min. Cells were then incubated in PBS containing 2% BSA for 30 min. Cells were then incubated with a 1/1000 dilution of the anti-HA monoclonal antibody AFC-101P (Covance) overnight at 4 °C. Cells were rinsed and incubated with Alexa Fluor 488-conjugated anti-mouse IgG (Life Technologies, A-11001) at 1/500 dilution for 30 min at room temperature to visualize immunocomplexes. Nuclei were stained with a 1/10,000 dilution of DAPI (Invitrogen, D-1306). Images were obtained using a Deltavision Personal DV microscope (Applied Precision). Where indicated, 0.5% saponin was added to permeabilize the plasma membrane.

Immunoprecipitations and SDS-PAGE—Transfected 293T cells from one 10-cm plate were lysed with 1 ml of immunoprecipitation buffer containing phosphatase inhibitors, immunoprecipitated with 3 μl of rabbit 6327 antiserum overnight, and fractionated on an 8% resolving gel as described previously (10).

Western Blotting—293T cells were transfected with the indicated constructs, and equal amounts of crude membranes were normalized to total protein, or immunoprecipitated complexes were fractionated by reducing SDS-PAGE and blotted to a Immobilon membrane for immunodetection as described previously (11). The blot was blocked and probed with a 1/5000 dilution of rabbit serum 6328 followed by incubation with a 1/20,000 dilution of goat anti-rabbit IRDye 680-conjugated antibody and visualized on a LI-COR instrument as described previously (31).

Gel Staining—Resolving gels were fixed in a 30-ml solution of 50% methanol and 10% acetic acid for 30 min with gentle rocking. The solution was changed once for a total of two washes in the fixing solution. The gels were then washed three times in 100 ml of water for 10 min. 10 ml of Pro-Q Diamond phosphoprotein gel stain was added, and gels were rocked for 1.5 h in the dark. The gels were then destained with 80 ml of a solution of 20% acetonitrile, 50 mM sodium acetate (pH 4.0) for 15 min three times. The gels were then rinsed in water and scanned with a 532-nm laser on a Typhoon FLA 9500 imager (GE Life Sciences) (32). After imaging, the gel was rinsed and stained with Coomassie Brilliant Blue.

Guanylyl Cyclase Assays—Crude membranes were prepared in phosphatase inhibitor buffer from 293T-GC-B cells as described previously (33). All assays were performed at 37 °C in a mixture containing 25 mM Hepes (pH 7.4), 50 mM NaCl, 0.1% BSA, 0.5 mM isobutylmethyl xanthine, 1 mM EDTA, 0.5 μM microcystin, 10 mg/ml creatine kinase, 5 mM creatine phosphate, and 5 mM $MgCl_2$. The time each reaction was incubated at 37 °C is indicated in the figure legends. Unless otherwise indicated, 1 mM ATP and 0.1 mM GTP were included in the reaction solutions. Reactions were initiated by adding 60 μl of prewarmed reaction mixture to 20 μl of crude membranes suspended in 20 μl of phosphatase inhibitor buffer alone (basal) or producing final concentrations of 1 μM CNP or 1% Triton X-100 and 5 mM $Mn^{2+}Cl_2$, which was substituted for $MgCl_2$. Reactions were stopped with 0.4 ml of ice-cold 50 mM sodium acetate buffer containing 5 mM EDTA. Cyclic GMP concentrations were determined by radioimmunoassay (34).

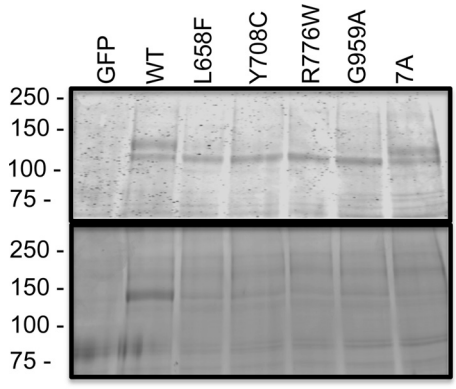

FIGURE 1. **AMDM mutants are not processed to the fully glycosylated and phosphorylated form of GC-B.** WT and the indicated missense versions of GC-B were isolated from transiently transfected 293T cells by sequential immunoprecipitation/SDS-PAGE purification. The resulting gel was incubated with ProQ Diamond dye to determine GC-B phosphate levels (*bottom panel*). The same gel was then washed and stained with Coomassie Brilliant Blue dye to determine the amount of GC-B protein present (*top panel*). Molecular mass in kilodaltons is shown for protein standards on the *left*. *7A*, GC-B containing alanine substitutions for all seven known phosphorylation sites. The figure is representative of three experiments.

^{125}I-CNP Binding Assays—Equal numbers of transiently transfected 293 cells were seeded in 24-well plates and grown to 70–90% confluence. Cells were incubated for 1 h in DMEM containing 0.2% BSA at 37 °C. Binding medium containing 1% BSA and 30 pM (20 nanocuries) of ^{125}I-CNP was added to each well and incubated at 4 °C for 1 h. For nonspecific binding wells, 1 μM of non-radioactive CNP was included in the binding buffer. For the competition binding assays, increasing concentrations of non-radioactive CNP were included in the binding buffer. The cells were washed with ice-cold PBS to remove nonspecifically bound ^{125}I-CNP. The cells were removed from the plate with 0.5 ml of 1 N NaOH, and the radioactivity of the cell extract was determined in a γ counter.

Tunicamycin Treatment—Four hours after 293T cells were transiently transfected, they were incubated with 2 μg/ml tunicamycin for 24 h, and then membranes were prepared in phosphatase inhibitor buffer for analysis.

Statistical Analysis—Statistics and graphs were generated with Prism 5 software. p Values were obtained using Student's paired t test, and $p \leq 0.05$ was considered significant. The error bars within the symbols represent standard error.

Results

AMDM Mutants Are Incompletely Processed—Posttranslational processing of four intracellular AMDM causing mutants (L658F, Y708C, R776W, and G959A) was compared with WT-GC-B and GC-B-7A, a mutant containing alanine substitutions for the seven known phosphorylation sites (9), in reduced SDS gels containing immunoprecipitated receptors from transiently transfected 293T cells. Coomassie staining (Fig. 1, *top panel*) of

WT-GC-B revealed a slower migrating, diffuse species (*top band*) that is maximally glycosylated and phosphorylated and a second, faster migrating species (*bottom band*) that is incompletely glycosylated and not phosphorylated. A fainter, fastest migrating form corresponding to the unprocessed polypeptide is visible in some lanes (Fig. 7) (8, 9). The upper band was also present in GC-B-7A, indicating that the majority of the migration difference between the two species is not due to changes in phosphorylation. In contrast, the upper band was markedly diminished or undetectable in samples from the AMDM mutants. ProQ Diamond staining, a dye that binds GC-B in a phosphate-dependent manner (32), of the same gel indicated that only the slower-migrating, upper species of the WT receptor was phosphorylated (Fig. 1, *bottom panel*).

The GC-B AMDM Mutants Bind CNP on the Surface of Cells—^{125}I-CNP binding assays were performed on live 293T cells transfected with the individual AMDM mutants, WT-GC-B as a positive control, and GFP as a negative control (Fig. 2, *top panel*). Low radiation levels in GFP-transfected cells and in GC-B-expressing cells exposed to excess non-radioactive CNP (nonspecific binding) confirmed that the binding was specific for GC-B. All four mutants specifically bound ^{125}I-CNP, consistent with GC-B being on the cell surface. Total ^{125}I-CNP binding to each mutant was variable and less than that observed for the WT receptor, which is expected because the mutants have reduced protein levels because of the lack of the completely processed and phosphorylated upper protein species only seen with WT-GC-B (Fig. 1, *top panel*). Competition binding assays indicated that the affinity of each mutant for CNP was similar to that of WT-GC-B (Fig. 2, *bottom panel*). These data indicate that all four mutants are on the cell surface and that glycosylation of GC-B is neither required to bind CNP nor required for GC-B to adopt a conformation capable of binding CNP.

Microscopic Detection Indicated That All Mutants Are on the Cell Surface—To verify that the mutants were on the cell surface, each mutation was introduced into an amino-terminally HA-tagged version of the human GC-B cDNA (35) and transiently expressed along with HA-WT-human GC-B in HeLa cells (Fig. 3). GC-B was detected by probing non-permeabilized and permeabilized cells with a monoclonal antibody to the extracellular HA epitope (Fig. 3, *green*). The plasma membrane was stained with wheat germ agglutinin (Fig. 3, *red*), and the nucleus was stained with DAPI (Fig. 3, *blue*). In the non-permeabilized cells (Fig. 3, *left panels*), no GC-B surface staining was observed on untransfected HeLa cells. However, a clear extracellular signal (Fig. 3, *green*) was detected for all receptors when probed with an antibody against the N-terminal GC-B HA epitope. Furthermore, the signal for the plasma membrane marker (Fig. 3, *red*) co-localized with all HA-tagged receptors (Fig. 3, *yellow*, *merged*). For cells permeabilized with saponin (Fig. 3, *right panels*), extracellular staining was more diffuse, and receptor staining was also observed in intracellular non-nuclear regions. Again, receptor staining colocalized with plasma membrane staining (Fig. 3, *yellow*). However, for the L658F and Y708C mutants, much more cytoplasmic staining was observed in the permeabilized cells than with the WT

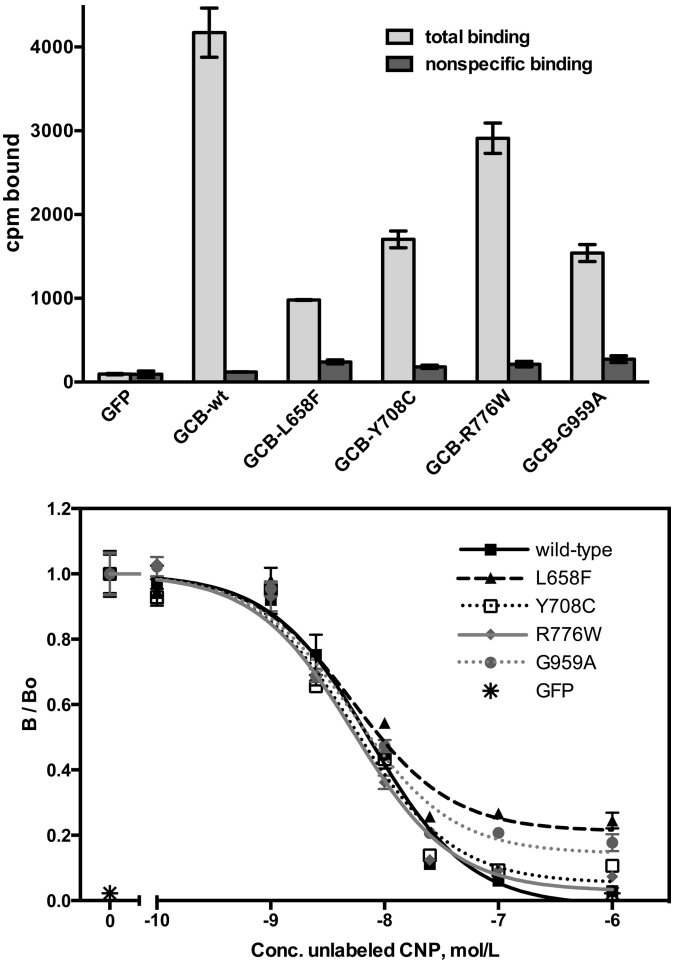

FIGURE 2. **The AMDM mutants bind ^{125}I-CNP on the surface of live cells.** 293 cells were transiently transfected with plasmids containing GFP, WT-GC-B, or the indicated mutants. Equal numbers of cells were seeded in the wells and then incubated for 1 h at 4 °C with 30 pM ^{125}I-CNP in the presence or absence of 1 μM (*top panel*) or increasing concentrations (*bottom panel*) of non-radioactive CNP. The cells were rinsed with binding medium to remove nonspecific ^{125}I-CNP, removed from the plate with NaOH, and subjected to γ counting to determine the amount of specifically bound ^{125}I-CNP. The *error bars* and *symbols* represent the standard error, where $n = 3$. *B/Bo* = specific binding over nonspecific binding; *conc.* = concentration.

enzyme or the R776W or G959A mutants. Together, these data verified that all mutants were on the cell surface.

AMDM Mutants Have Severely Reduced Guanylyl Cyclase Activity—The ability of the GC-B mutants to form active catalytic domains was examined in membranes from transfected 293 cells (Fig. 4). GC activity was measured under basal, CNP-stimulated, and detergent and manganese-stimulated conditions. The latter condition activates the enzyme independently of NP or phosphorylation and is an excellent indicator of total activated GC-B catalytic domain formation (9). CNP increased the activity of WT-GC-B 568-fold over basal levels but only increased the activity of GC-B-G959A 36-fold and completely failed to activate the other three mutants. Triton X-100 and manganese increased WT-GC-B activity 704-fold over basal levels, but the AMDM causing mutant forms of GC-B were activated by detergent to less than 16% of WT levels. In contrast, the mutations had no effect on basal GC activity.

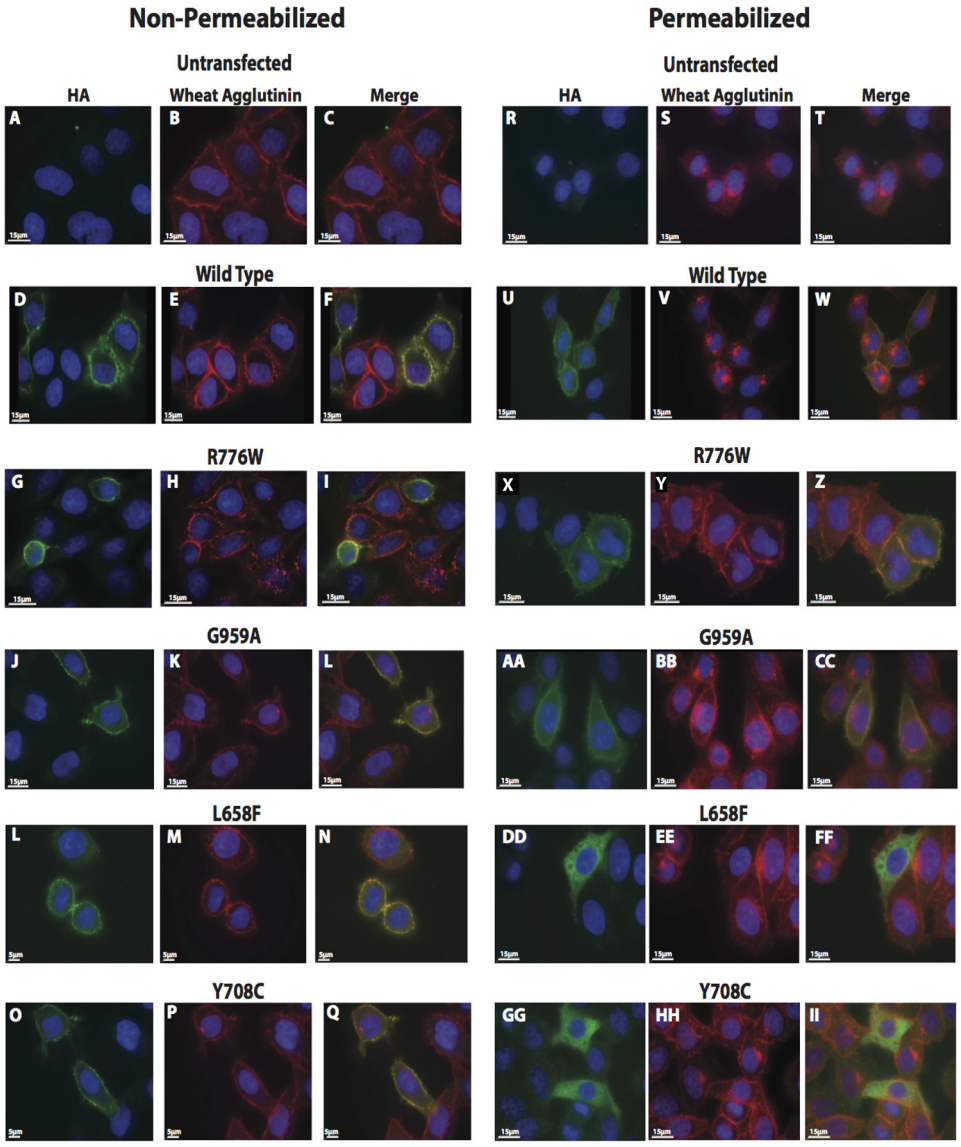

FIGURE 3. **Microscopic immunofluorescence detection indicates that the AMDM mutants are on the cell surface.** HeLa cells were transiently transfected with HA-tagged WT-GC-B, the indicated HA-tagged ADMA mutants, or no plasmid DNA. Cells were fixed and stained as described under "Experimental Procedures" and then visualized using a Deltavision Personal DV microscope (Applied Precision). *A*, *D*, *G*, *J*, *L*, and *O*, non-permeabilized staining using an antibody against the HA epitope (*green*). *B*, *E*, *H*, *K*, *M*, and *P*, non-permeabilized plasma membrane staining using wheat agglutinin 594 (*red*). *C*, *F*, *I*, *L*, *N*, and *Q*, non-permeabilized colocalization of the HA-stain and plasma membrane stain (*yellow*). *R*, *U*, *X*, *AA*, *DD*, and *GG*, permeabilized staining using an antibody against the HA epitope (*green*). *S*, *V*, *Y*, *BB*, *EE*, and *HH*, permeabilized plasma membrane staining using wheat agglutinin 594 (*red*). *T*, *W*, *Z*, *CC*, *FF*, and *II*, permeabilized colocalization of the HA stain and plasma membrane stain (*yellow*).

Lack of Phosphorylation Does Not Explain the Inactivity of the AMDM Mutants—Because phosphorylation is required for CNP-dependent activation of GC-B (9), we tested whether lack of phosphorylation caused the mutant enzymes to be inactive. If this hypothesis was true, then the mutations should fail to inactivate a "constitutively phosphorylated" form of the enzyme, known as GC-B-7E, that contains glutamate substitutions for the seven known phosphorylation sites (13). Introduction of the AMDM mutations in a plasmid expressing GC-B-7E resulted in incompletely processed enzymes that bind CNP on the cell surface but lack GC activity, as observed when the mutations were examined in the WT phosphorylated form of GC-B (Fig. 5). These data indicate that the AMDM mutation-dependent loss in GC activity is independent of GC-B phosphorylation.

Blocking Glycosylation in the ER Inhibits CNP- and Detergent-stimulated Guanylyl Cyclase Activity—To test the effect of blocking ER mediated glycosylation on GC-B activity, WT-GC-B, GC-B-7E, GC-B-L658F, and GC-B-G959A were transfected in 293T cells in duplicate and incubated with or without tunicamycin, a chemical that inhibits the rate-limiting step of *N*-linked glycosylation in the ER (36). Western blotting indicated that tunicamycin inhibited glycosylation of GC-B at a very early stage because cells treated with the drug only produced the fastest-migrating, unmodified doublet species and lacked the fainter upper most active species denoted by the *large arrowhead* in Fig. 6*B*. We have never seen the doublet lower species before but hypothesize that it represents the naked polypeptide chain of GC-B with and without the signal

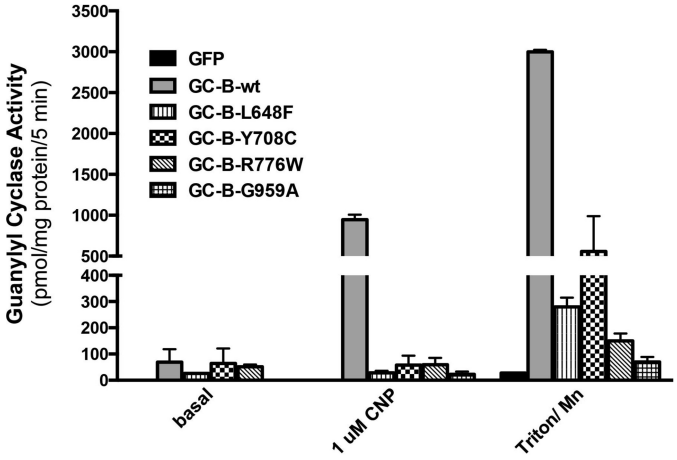

FIGURE 4. **The AMDM mutants have markedly reduced activated guanylyl cyclase activity.** 293T cells were transiently transfected with plasmids containing GFP, WT-GC-B, or the indicated GC-B mutants. Crude membranes were prepared from the transfected cells and assayed for guanylyl cyclase activity under basal, CNP-stimulated, or Triton X-100 and manganese-stimulated conditions. The *error bars* represent the standard error, where $n = 6$ from three experiments.

peptide sequence, although we cannot rule out the possibility that it results from palmitoylation (37). Consistent with glycosylation being required for the formation of a stimulated catalytic domain, CNP- and detergent-dependent guanylyl cyclase activities of the WT and mutant GC-B enzymes were dramatically reduced by tunicamycin treatment, whereas basal activity was unaffected. The reduction in stimulated activity was much greater for WT-GC-B and GC-B-7E because these enzymes were more glycosylated in the absence of tunicamycin (Fig. 6*B*, *top arrowhead*) compared with GC-B-L658F and GC-B-G959A.

Mutation of the Asn-24 Glycosylation Site Reduces Guanylyl Cyclase Activity—Mutagenesis studies identified five *N*-linked glycosylation sites in GC-B, and the one that had the greatest effect on migration was Asn-24 (38). Therefore, we mutated Asn-24 to Asp or Gln in WT-GC-B and the L658F AMDM mutant and assessed the guanylyl cyclase activity of the resulting enzymes in membranes from transfected 293 cells (Fig. 7). As expected, both Asp and Gln substitutions for Asn-24 reduced CNP and detergent-dependent GC activity as well as the slower migrating form of GC-B when introduced into the WT-GC-B backbone. However, the activity reduction observed for GC-B-L658F was greater than that observed for either Asn-24 mutation, which is expected given that the L658F mutant likely is missing multiple glycosylation sites based on the large increase in electrophoretic mobility compared with the WT enzyme. Importantly, ablating the Asn-24 glycosylation site did not increase the electrophoretic migration of the GC-B-L658F mutant, consistent with this mutant lacking glycosylation at that site.

Blocking Glycosylation in the Golgi Apparatus Does Not Inhibit GC Activity—To test the effect of Golgi-dependent glycosylation on guanylyl cyclase activity, WT-GC-B was expressed in regular 293T cells and a mutant 293 cell line lacking the Golgi enzyme, *N*-acetylglucosaminyltransferase I (Gnt1$^-$). This enzyme adds complex sugars to proteins that have been trimmed of high mannose sugars added in the ER

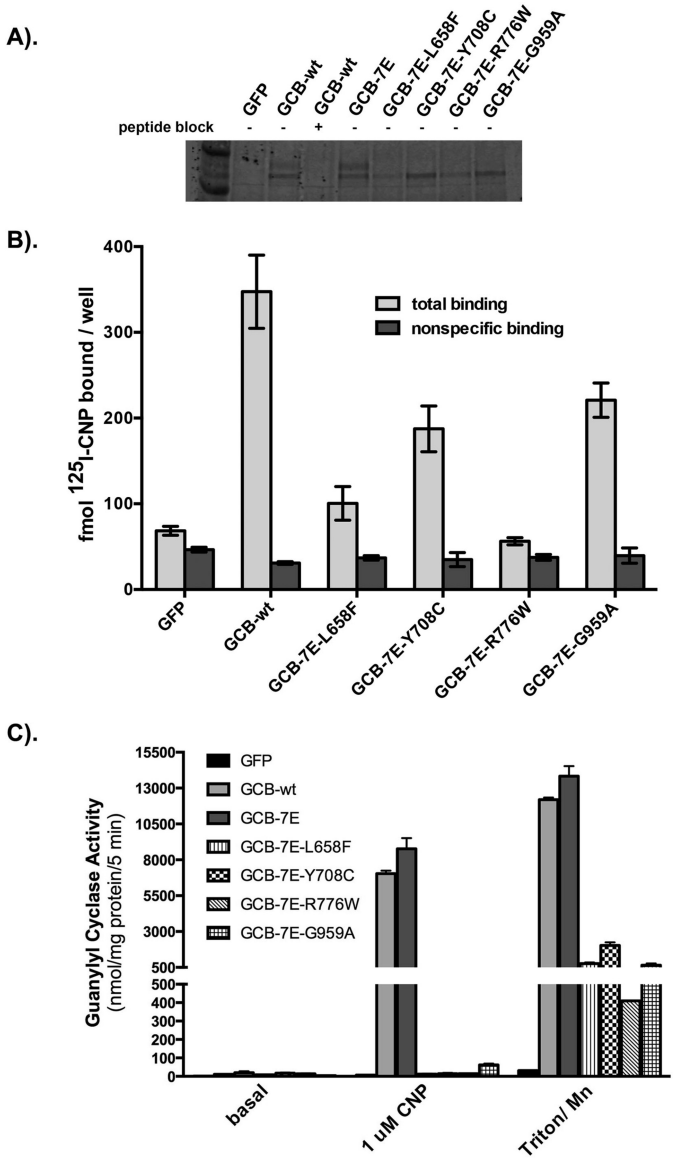

FIGURE 5. **Reduced phosphorylation does not explain the inactivation of the AMDM mutants.** 293T cells were transiently transfected with plasmids encoding GFP, WT-GC-B, or the indicated GC-B mutants. *A*, GC-B proteins were isolated by sequential immunoprecipitation/SDS-PAGE purification followed by Western blotting detection. *Peptide block* indicates that the peptide antigen was or was not included in the immunoprecipitation reaction to specifically block binding to GC-B. *B*, equal numbers of cells were incubated for 1 h at 4 °C with 30 pM ^{125}I-CNP in the presence or absence of non-radioactive CNP. The cells were rinsed with binding medium to remove nonspecific ^{125}I-CNP, removed from the plate with NaOH, and subjected to γ counting to determine the amount of specifically bound ^{125}I-CNP. The *error bars* represent the standard error, where $n = 3$. *C*, crude membranes were prepared from the transfected cells and assayed for guanylyl cyclase activity under the indicated conditions. The *error bars* represent the standard error, where $n = 5$ from three experiments.

(Fig. 8). WT-GC-B isolated from the Gnt1$^-$ cells lacked the fully processed, slowest migrating (upper) species and showed an increase in the incompletely processed middle form. However, total expression of GC-B in the Gnt1$^-$ cells was similar to total GC-B expression in the 293T cells that express the Gnt1 I gene (Fig. 8, *top panel*). Importantly, CNP-stimulated and detergent-stimulated activities were similar regardless of Gnt1 gene expression and Golgi-dependent glycosylation of GC-B.

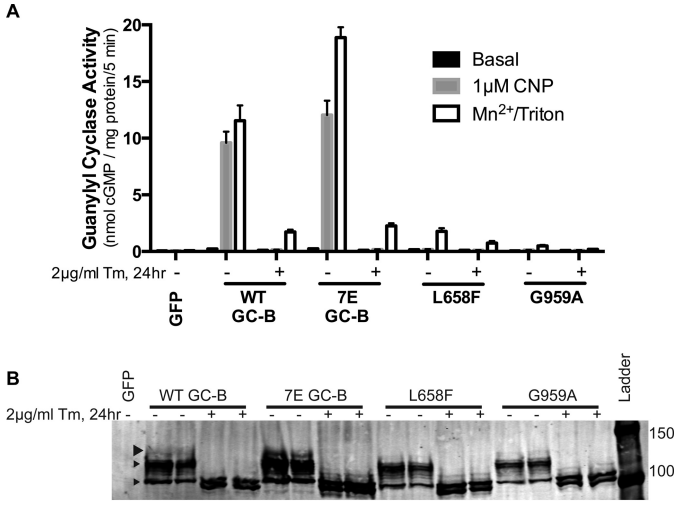

FIGURE 6. ***N*-linked glycosylation in the ER is required for stimulated GC-B activity.** *A* and *B*, 293T cells were transiently transfected with plasmids encoding GFP, WT-GC-B, GC-B-7E, GC-B-L658F, or GC-B-G959A and incubated in the presence (+) or absence (−) of tunicamycin before preparing membranes and assaying them for guanylyl cyclase activity under the condition shown (*top panel*) or changes in molecular mass by sequential immunoprecipitation and Western blotting analysis (*bottom panel*). The *error bars* represent the range of duplicate determination. The Western blot is representative of three individual experiments. The GC results shown are representative of four similar experiments. *Arrowheads* indicate the three commonly observed electrophoretic forms of GC-B, with the *large arrowhead* representing the most highly glycosylated and active form.

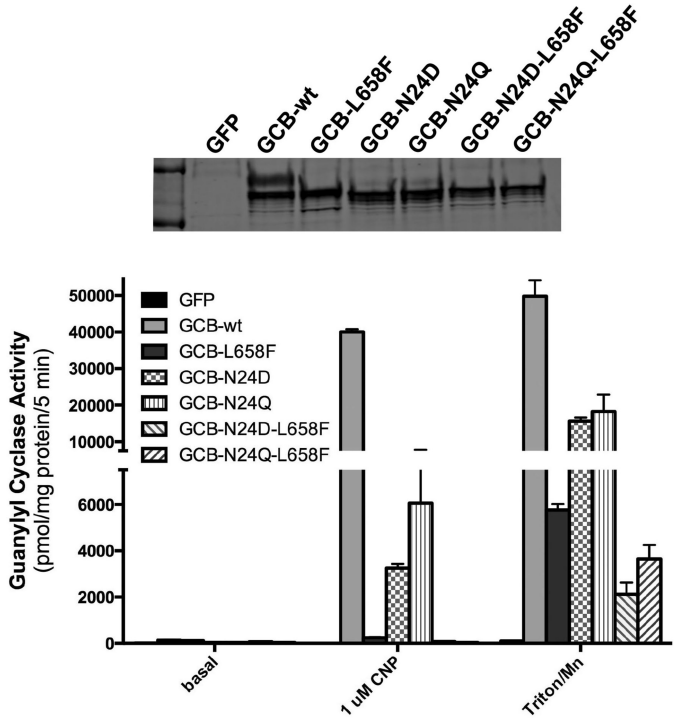

FIGURE 7. **Mutation of the Asn-24 glycosylation site decreases the guanylyl cyclase activity and increases the electrophoretic migration of GC-B.** 293T cells were transiently transfected with plasmids containing GFP, WT-GC-B, or the indicated GC-B mutants. Crude membranes were prepared from the transfected cells, and GC-B migration was analyzed by Western blotting analysis (*top panel*) or assayed for guanylyl cyclase activity (*bottom panel*) under basal, CNP-stimulated, or Triton X-100 and manganese-stimulated conditions. The *error bars* represent the standard deviation, where $n = 4$ and is representative of three experiments.

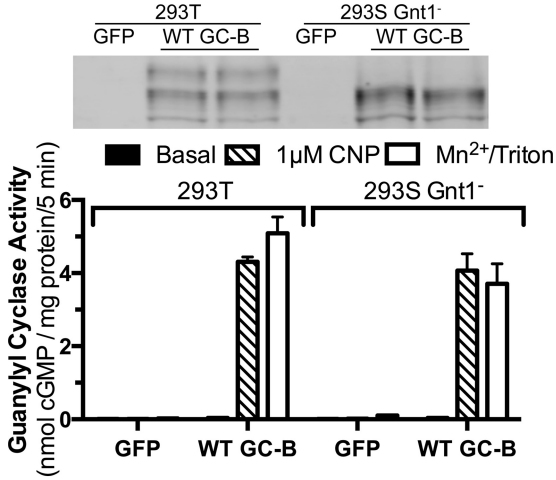

FIGURE 8. **Incomplete glycosylation in the Golgi apparatus does not reduce CNP- or detergent-dependent guanylyl cyclase activity of GC-B.** A plasmid expressing WT-GC-B was transiently transfected into 293T or 293S Gnt1$^-$ cells. GC-B was then purified by sequential immunoprecipitation and SDS-PAGE and detected by Western blotting (*top panel*), or membranes were prepared from these cells and assayed for guanylyl cyclase activity under the indicated conditions. The *error bars* represent the standard error, where $n = 4$. The experiment is representative of three similar experiments.

Enzymatic Deglycosylation of Fully Processed GC-B Does Not Reduce Enzymatic Activity—Finally, WT and mutant enzymes immunoprecipitated and bound to protein-A-agarose beads were incubated with or without PNGase F, which cleaves the covalent bond between the innermost GlcNAc and asparagine of the enzyme. The receptors were then purified by SDS-PAGE and visualized by Western blotting or assayed for guanylyl cyclase activity in the presence of Mn^{2+}GTP and Triton X-100 (Fig. 9, *top panels*). The electrophoretic migration of the WT enzyme increased the most because it was more highly glycosylated. However, the electrophoretic mobility of the mutants also increased because they were partially glycosylated. Importantly, the electrophoretic mobility of the PNGase F-treated WT enzyme was the same as the mobility of the PNGase F-treated mutants. Thus, deglycosylation completely explains the increased migration of the mutant enzymes. However, PNGase F had no effect on the guanylyl cyclase activity of the WT or mutant enzymes.

To evaluate the effect of deglycosylation on CNP-dependent activity, membranes from 293T cells transfected with WT-GC-B were incubated with PNGase F and then assayed for CNP- and detergent-dependent GC activity or purified by immunoprecipitation and SDS-PAGE. The appearance of a faster-migrating species indicated that 12.2% of the total amount of GC-B was deglycosylated, and the corresponding decrease in the second band indicated that only the incompletely glycosylated form of GC-B was cleaved by PNGase F in membranes. Incomplete deglycosylation in the membranes compared with purified GC-B bound to protein-A-agarose is expected because the membranes contain more substrates for PNGase F. Nonetheless, no reduction in GC activity measured under CNP or detergent conditions was observed in membranes that were exposed to PNGase F, which is expected given that the upper completely glycosylated and active species was not cleaved. Taken together, these data are consistent with a

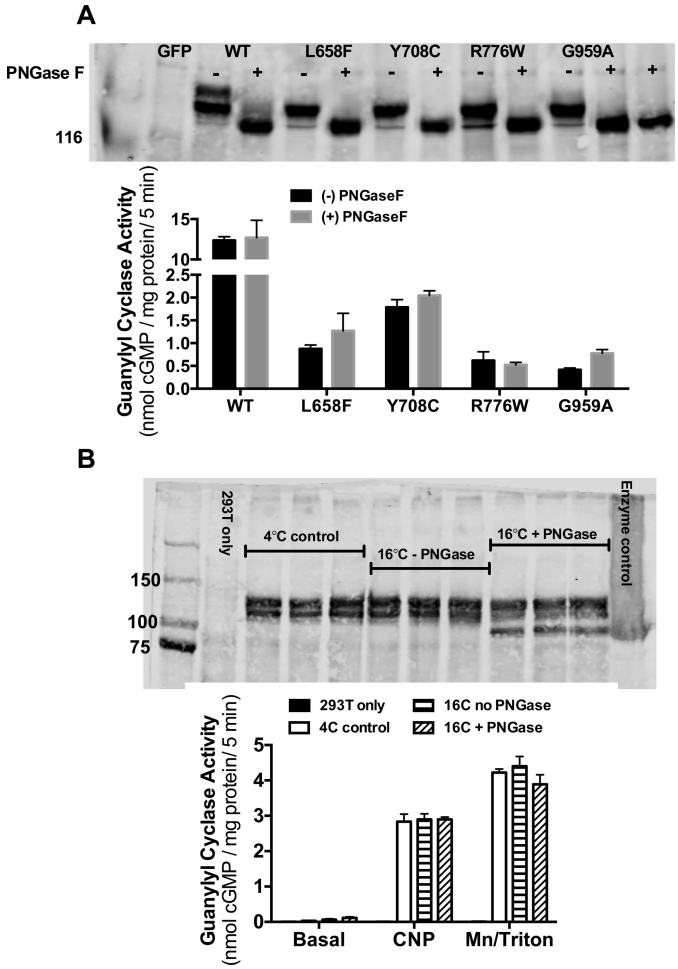

FIGURE 9. **Enzymatic deglycosylation after normal processing does not inhibit GC-B activity.** *A*, crude membranes were prepared from 293T cells stably expressing GC-B, and then GC-B was immunoprecipitated and incubated with or without PNGase F for 15 min at 16 °C. SDS-PAGE-purified receptors were Western-blotted to verify deglycosylation. Guanylyl cyclase activity was assayed in the presence of Mn^{2+}GTP and Triton X-100. *B*, crude membranes were treated with or without PNGase F for 15 min at 16 °C and then Western-blotted or assayed for guanylyl cyclase activity as indicated. The enzyme control was from crude membranes that were first denatured by boiling and then treated with PNGase F for 1 h at 37 °C. The total amount of GC-B (*center band*) cleaved was determined by analyzing the scanned image with ImageJ software.

model where *N*-linked glycosylation in the ER is required for proper folding of the catalytic but not the NP-binding domain of GC-B. However, when folded, terminal glycosylation is no longer required to produce a stimulated catalytic unit.

Discussion

Posttranslational modifications regulate the activity and location of proteins. Here we report that glycosylation is required for the formation of an activated catalytic domain but that it does not regulate the cellular location of GC-B or its ability to bind CNP. Importantly, we connect mutations that result in deglycosylated forms of GC-B to a disease for the first time.

Previous studies on the role of glycosylation on GC-A and GC-B were conflicting. Incompletely glycosylated GC-A was initially reported to lack the ability to bind ^{125}I-ANP (39). In contrast, Miyagi *et al.* (40) identified five *N*-linked glycosylation sites in GC-A but found that glycosylation was not required for ANP binding . A third report demonstrated that incompletely glycosylated mutants of GC-A bound but could not be activated by ANP (41). Regarding GC-B, mutagenesis of five of the seven potential *N*-linked glycosylation sites in the bovine receptor revealed that Asn-24 is a conserved glycosylation site and that mutagenesis of this site inhibits CNP-dependent cGMP elevations but does not affect the affinity of CNP for the membrane-exposed receptor (38). Here we determined that the single Asn-24 mutation decreased both the CNP- and detergent-dependent activity of GC-B, consistent with the notion of glycosylation being required for maximum enzymatic activity of GC-B. Our data are consistent with the majority of previously published observations showing that reduced glycosylation of GC-A and GC-B decreases cGMP generation but not natriuretic peptide binding.

Experiments employing tunicamycin and *N*-acetylglucosaminyltransferase I-deficient cells allowed the effects of GC-B glycosylation in the ER *versus* the Golgi apparatus to be tested independently of the AMDM mutations. Because only tunicamycin treatment decreased catalytic activity, we conclude that glycosylation in the ER is required for the catalytic domain to fold into an active conformation, consistent with glycosylation increasing the solubility and chaperone binding of proteins (42). In contrast, neither blocking terminal glycosylation in the Golgi nor enzymatically removing sugar residues from the completely processed enzyme reduced the activity of GC-B. Interestingly, because the level of the lower, more rapidly migrating species of GC-B is unchanged between the WT and mutant enzymes, this suggests that the mutants are selectively degraded in a membrane-limited compartment of the cell, possibly by the incompletely glycosylated form being exported out of the ER and degraded in the cytoplasm.

A previous study using site-directed mutants correlated deglycosylated forms of GC-A with decreased guanylyl cyclase activity. However, because these mutants were also dephosphorylated, whether the loss of activity was due to lack of glycosylation or phosphorylation could not be determined (41). Our experiments employing the constitutively phosphorylated GC-B-7E enzyme allowed the effects of phosphorylation and glycosylation to be separated for the first time. When inactivating AMDM mutations were engineered into a GC-B-7E backbone, the resultant enzymes were inactive. As a result of this report, we can now say that both processes are required for activation of GC-B, with each modification having a different purpose. Phosphorylation is required for transduction of the NP binding signal to the catalytic domain but not required for glycosylation, and it does not affect the formation of functional ligand binding or catalytic domains (9, 43). In contrast, glycosylation is required for formation of a stimulated catalytic domain because prevention of glycosylation in the ER inhibits NP- and detergent-dependent but not basal GC activity.

Immunofluorescence imaging studies on mutant forms of GC-B in the initial AMDM report led to the conclusion that the mutations disrupted targeting of GC-B to the cell surface (25). However, Amano *et al.* (24) subsequently showed that the Q417E dwarfism mutation did not affect surface expression of GC-B. Positive detection by Amano *et al.* (24) is likely explained

by their use of an N-terminal *versus* C-terminal HA GC-B tag, which allowed surface protein detection in the absence of membrane-permeating agents. Our ^{125}I-CNP binding and immunofluorescence experiments on live cells clearly indicated that all four mutants are on the cell surface. The immunofluorescence data also indicated that the L658F and Y708C mutants have a partial trafficking defect, although this did not explain the loss of GC activity. Consistent with our results, Hachiya *et al.* (16) found that HA-tagged-GC-B-L658F bound ^{125}I-CNP when expressed in whole cells but lacked GC activity. Finally, we point out that, of the three bands commonly seen for GC-B on Western blots, it is only the uppermost band that correlates with guanylyl cyclase activity. Hence, in future studies, only the upper band should be measured when investigating the GC activity of the enzyme.

We conclude that ER-mediated glycosylation is required for CNP- and detergent-stimulated catalytic activity of GC-B. Furthermore, we report that four unique AMDM missense mutants produce a conformation that is incompatible with ER-mediated glycosylation and result in proteins that bind CNP on the cell surface but lack stimulated guanylyl cyclase activity. Thus, our data refute the current "defective trafficking" hypothesis to explain the lack of activity of AMDM mutants. Finally, we predict that any homozygous mutation that inhibits ER-mediated glycosylation of GC-B will inactivate the enzyme and result in skeletal undergrowth.

Author Contributions—D. M. D. and A. B. E. conceived and performed the experiments and wrote the paper. N. M. O., T. S. C., and J. W. R. performed the experiments and edited the paper. L. R. P. conceived and coordinated the study and wrote the paper.

Acknowledgment—We thank Dr. Laurinda Jaffe for helpful comments on this manuscript.

References

1. Potter, L. R. (2011) Natriuretic peptide metabolism, clearance and degradation. *FEBS J.* **278,** 1808–1817
2. Potter, L. R. (2011) Regulation and therapeutic targeting of peptide-activated receptor guanylyl cyclases. *Pharmacol. Ther.* **130,** 71–82
3. Potter, L. R. (2011) Guanylyl cyclase structure, function and regulation. *Cell. Signal.* **23,** 1921–1926
4. Tamura, N., Doolittle, L. K., Hammer, R. E., Shelton, J. M., Richardson, J. A., and Garbers, D. L. (2004) Critical roles of the guanylyl cyclase B receptor in endochondral ossification and development of female reproductive organs. *Proc. Natl. Acad. Sci. U.S.A.* **101,** 17300–17305
5. Schmidt, H., Stonkute, A., Jüttner, R., Schäffer, S., Buttgereit, J., Feil, R., Hofmann, F., and Rathjen, F. G. (2007) The receptor guanylyl cyclase Npr2 is essential for sensory axon bifurcation within the spinal cord. *J. Cell Biol.* **179,** 331–340
6. Zhang, M., Su, Y. Q., Sugiura, K., Xia, G., and Eppig, J. J. (2010) Granulosa cell ligand NPPC and its receptor NPR2 maintain meiotic arrest in mouse oocytes. *Science* **330,** 366–369
7. Potter, L. R., and Hunter, T. (2001) Guanylyl cyclase-linked natriuretic peptide receptors: structure and regulation. *J. Biol. Chem.* **276,** 6057–6060
8. Potter, L. R. (1998) Phosphorylation-dependent regulation of the guanylyl cyclase-linked natriuretic peptide receptor B: dephosphorylation is a mechanism of desensitization. *Biochemistry* **37,** 2422–2429
9. Potter, L. R., and Hunter, T. (1998) Identification and characterization of the major phosphorylation sites of the B-type natriuretic peptide receptor. *J. Biol. Chem.* **273,** 15533–15539
10. Potthast, R., Abbey-Hosch, S. E., Antos, L. K., Marchant, J. S., Kuhn, M., and Potter, L. R. (2004) Calcium-dependent dephosphorylation mediates the hyperosmotic and lysophosphatidic acid-dependent inhibition of natriuretic peptide receptor-B/guanylyl cyclase-B. *J. Biol. Chem.* **279,** 48513–48519
11. Abbey-Hosch, S. E., Smirnov, D., and Potter, L. R. (2005) Differential regulation of NPR-B/GC-B by protein kinase c and calcium. *Biochem. Pharmacol.* **70,** 686–694
12. Yoder, A. R., Stone, M. D., Griffin, T. J., and Potter, L. R. (2010) Mass spectrometric identification of phosphorylation sites in guanylyl cyclase a and B. *Biochemistry* **49,** 10137–10145
13. Yoder, A. R., Robinson, J. W., Dickey, D. M., Andersland, J., Rose, B. A., Stone, M. D., Griffin, T. J., and Potter, L. R. (2012) A functional screen provides evidence for a conserved, regulatory, juxtamembrane phosphorylation site in guanylyl cyclase A and B. *PLoS ONE* **7,** e36747
14. Shuhaibar, L. C., Egbert, J. R., Edmund, A. B., Uliasz, T. F., Dickey, D. M., Yee, S. P., Potter, L. R., and Jaffe, L. A. (2016) Dephosphorylation of juxtamembrane serines and threonines of the NPR2 guanylyl cyclase is required for rapid resumption of oocyte meiosis in response to luteinizing hormone. *Dev. Biol.* **409,** 194–201
15. Bartels, C. F., Bükülmez, H., Padayatti, P., Rhee, D. K., van Ravenswaaij-Arts, C., Pauli, R. M., Mundlos, S., Chitayat, D., Shih, L. Y., Al-Gazali, L. I., Kant, S., Cole, T., Morton, J., Cormier-Daire, V., Faivre, L., Lees, M., Kirk, J., Mortier, G. R., Leroy, J., Zabel, B., Kim, C. A., Crow, Y., Braverman, N. E., van den Akker, F., and Warman, M. L. (2004) Mutations in the transmembrane natriuretic peptide receptor NPR-B impair skeletal growth and cause acromesomelic dysplasia, type Maroteaux. *Am. J. Hum. Genet.* **75,** 27–34
16. Hachiya, R., Ohashi, Y., Kamei, Y., Suganami, T., Mochizuki, H., Mitsui, N., Saitoh, M., Sakuragi, M., Nishimura, G., Ohashi, H., Hasegawa, T., and Ogawa, Y. (2007) Intact kinase homology domain of natriuretic peptide receptor-B is essential for skeletal development. *J. Clin. Endocrinol. Metab.* **92,** 4009–4014
17. Khan, S., Ali, R. H., Abbasi, S., Nawaz, M., Muhammad, N., and Ahmad, W. (2012) Novel mutations in natriuretic peptide receptor-2 gene underlie acromesomelic dysplasia, type Maroteaux. *BMC Med. Genet.* **13,** 44
18. Wang, S. R., Jacobsen, C. M., Carmichael, H., Edmund, A. B., Robinson, J. W., Olney, R. C., Miller, T. C., Moon, J. E., Mericq, V., Potter, L. R., Warman, M. L., Hirschhorn, J. N., and Dauber, A. (2015) Heterozygous mutations in natriuretic peptide receptor-B (NPR2) gene as a cause of short stature. *Hum. Mutat.* **36,** 474–481
19. Olney, R. C., Bükülmez, H., Bartels, C. F., Prickett, T. C., Espiner, E. A., Potter, L. R., and Warman, M. L. (2006) Heterozygous mutations in natriuretic peptide receptor-B (NPR2) are associated with short stature. *J. Clin. Endocrinol. Metab.* **91,** 1229–1232
20. Hisado-Oliva, A., Garre-Vázquez, A. I., Santaolalla-Caballero, F., Belinchón, A., Barreda-Bonis, A. C., Vasques, G. A., Ramirez, J., Luzuriaga, C., Carlone, G., González-Casado, I., Benito-Sanz, S., Jorge, A. A., Campos-Barros, A., and Heath, K. E. (2015) Heterozygous NPR2 mutations cause disproportionate short stature, similar to Leri-Weill dyschondrosteosis. *J. Clin. Endocrinol. Metab.* **100,** E1133–E1142
21. Hannema, S. E., van Duyvenvoorde, H. A., Premsler, T., Yang, R. B., Mueller, T. D., Gassner, B., Oberwinkler, H., Roelfsema, F., Santen, G. W., Prickett, T., Kant, S. G., Verkerk, A. J., Uitterlinden, A. G., Espiner, E., Ruivenkamp, C. A., Oostdijk, W., Pereira, A. M., Losekoot, M., Kuhn, M., and Wit, J. M. (2013) An activating mutation in the kinase homology domain of the natriuretic peptide receptor-2 causes extremely tall stature without skeletal deformities. *J. Clin. Endocrinol. Metab.* **98,** E1988–1998
22. Miura, K., Kim, O. H., Lee, H. R., Namba, N., Michigami, T., Yoo, W. J., Choi, I. H., Ozono, K., and Cho, T. J. (2014) Overgrowth syndrome associated with a gain-of-function mutation of the natriuretic peptide receptor 2 (NPR2) gene. *Am. J. Med. Genet. A* **164A,** 156–163
23. Miura, K., Namba, N., Fujiwara, M., Ohata, Y., Ishida, H., Kitaoka, T., Kubota, T., Hirai, H., Higuchi, C., Tsumaki, N., Yoshikawa, H., Sakai, N., Michigami, T., and Ozono, K. (2012) An overgrowth disorder associated with excessive production of cGMP due to a gain-of-function mutation of the natriuretic peptide receptor 2 gene. *PLoS ONE* **7,** e42180
24. Amano, N., Mukai, T., Ito, Y., Narumi, S., Tanaka, T., Yokoya, S., Ogata, T.,

and Hasegawa, T. (2014) Identification and functional characterization of two novel NPR2 mutations in Japanese patients with short stature. *J. Clin. Endocrinol. Metab.* **99,** E713–718
25. Hume, A. N., Buttgereit, J., Al-Awadhi, A. M., Al-Suwaidi, S. S., John, A., Bader, M., Seabra, M. C., Al-Gazali, L., and Ali, B. R. (2009) Defective cellular trafficking of missense NPR-B mutants is the major mechanism underlying acromesomelic dysplasia-type Maroteaux. *Hum. Mol. Genet.* **18,** 267–277
26. Vasques, G. A., Amano, N., Docko, A. J., Funari, M. F., Quedas, E. P., Nishi, M. Y., Arnhold, I. J., Hasegawa, T., and Jorge, A. A. (2013) Heterozygous mutations in natriuretic peptide receptor-B (NPR2) gene as a cause of short stature in patients initially classified as idiopathic short stature. *J. Clin. Endocrinol. Metab.* **98,** E1636–1644
27. Wang, W., Song, M. H., Miura, K., Fujiwara, M., Nawa, N., Ohata, Y., Kitaoka, T., Kubota, T., Namba, N., Jin, D. K., Kim, O. H., Ozono, K., and Cho, T. J. (2016) Acromesomelic dysplasia, type Maroteaux caused by novel loss-of-function mutations of the NPR2 gene: three case reports. *Am. J. Med. Genet. A* **170,** 426–434
28. Fan, D., Bryan, P. M., Antos, L. K., Potthast, R. J., and Potter, L. R. (2005) Down-regulation does not mediate natriuretic peptide-dependent desensitization of natriuretic peptide receptor (NPR)-A or NPR-B: guanylyl cyclase-linked natriuretic peptide receptors do not internalize. *Mol. Pharmacol.* **67,** 174–183
29. Reeves, P. J., Callewaert, N., Contreras, R., and Khorana, H. G. (2002) Structure and function in rhodopsin: high-level expression of rhodopsin with restricted and homogeneous *N*-glycosylation by a tetracycline-inducible *N*-acetylglucosaminyltransferase I-negative HEK293S stable mammalian cell line. *Proc. Natl. Acad. Sci. U.S.A.* **99,** 13419–13424
30. Robinson, J. W., and Potter, L. R. (2012) Guanylyl cyclases A and B are asymmetric dimers that are allosterically activated by ATP binding to the catalytic domain. *Sci. Signal.* **5,** ra65
31. Flora, D. R., and Potter, L. R. (2010) Prolonged atrial natriuretic peptide exposure stimulates guanylyl cyclase-A degradation. *Endocrinology* **151,** 2769–2776
32. Bryan, P. M., Smirnov, D., Smolenski, A., Feil, S., Feil, R., Hofmann, F., Lohmann, S., and Potter, L. R. (2006) A sensitive method for determining the phosphorylation status of natriuretic peptide receptors: cGK-Iα does not regulate NPR-A. *Biochemistry* **45,** 1295–1303
33. Robinson, J. W., and Potter, L. R. (2011) ATP potentiates competitive inhibition of guanylyl cyclase A and B by the staurosporine analog, Go6976: reciprocal regulation of ATP and GTP binding. *J. Biol. Chem.* **286,** 33841–33844
34. Abbey, S. E., and Potter, L. R. (2002) Vasopressin-dependent inhibition of the C-type natriuretic peptide receptor, NPR-B/GC-B, requires elevated intracellular calcium concentrations. *J. Biol. Chem.* **277,** 42423–42430
35. Robinson, J. W., Dickey, D. M., Miura, K., Michigami, T., Ozono, K., and Potter, L. R. (2013) A human skeletal overgrowth mutation increases maximal velocity and blocks desensitization of guanylyl cyclase-B. *Bone* **56,** 375–382
36. Prescher, J. A., and Bertozzi, C. R. (2006) Chemical technologies for probing glycans. *Cell* **126,** 851–854
37. Patterson, S. I., and Skene, J. H. (1994) Novel inhibitory action of tunicamycin homologues suggests a role for dynamic protein fatty acylation in growth cone-mediated neurite extension. *J. Cell Biol.* **124,** 521–536
38. Fenrick, R., Bouchard, N., McNicoll, N., and De Léan, A. (1997) Glycosylation of asparagine 24 of the natriuretic peptide receptor-B is crucial for the formation of a competent ligand binding domain. *Mol. Cell Biochem.* **173,** 25–32
39. Lowe, D. G., and Fendly, B. M. (1992) Human natriuretic peptide receptor-A guanylyl cyclase: hormone cross- linking and antibody reactivity distinguish receptor glycoforms. *J. Biol. Chem.* **267,** 21691–21697
40. Miyagi, M., Zhang, X., and Misono, K. S. (2000) Glycosylation sites in the atrial natriuretic peptide receptor oligosaccharide structures are not required for hormone binding. *Eur. J. Biochem.* **267,** 5758–5768
41. Koller, K. J., Lipari, M. T., and Goeddel, D. V. (1993) Proper glycosylation and phosphorylation of the type A natriuretic peptide receptor are required for hormone-stimulated guanylyl cyclase activity. *J. Biol. Chem.* **268,** 5997–6003
42. Tannous, A., Pisoni, G. B., Hebert, D. N., and Molinari, M. (2015) *N*-linked sugar-regulated protein folding and quality control in the ER. *Semin. Cell Dev. Biol.* **41,** 79–89
43. Potter, L. R., and Hunter, T. (1998) Phosphorylation of the kinase homology domain is essential for activation of the A-type natriuretic peptide receptor. *Mol. Cell. Biol.* **18,** 2164–2172